

Effects of visible and UV light on the characteristics and properties of crude oil-in-water (O/W) emulsions†

Homer C. Genuino,^a Dayton T. Horvath,^a Cecil K. King'ondu,^a George E. Hoag,^b John B. Collins^b and Steven L. Suib*^a

Received 30th August 2011, Accepted 22nd December 2011

DOI: 10.1039/c2pp05275j

The effects of visible and UV light on the characteristics and properties of Prudhoe Bay (PB) and South Louisiana (SL) emulsions were investigated to better understand the role of sunlight on the fate of spilled crude oils that form emulsions with a dispersant in the aquatic environment. Before irradiation, crude oil emulsions showed the presence of dispersed crude oil micelles in a continuous water phase and crude oil components floating on the surface. The crude oil micelles decreased in size with irradiation, but emulsions retained their high degree of polydispersity. UV irradiation reduced the stability of emulsions more effectively than visible light. The reduction of micelles size caused the viscosity of emulsions to increase and melting point to decrease. Further, irradiation increased acid concentrations and induced ion formation which lowered the pH and increased the conductivity of emulsions, respectively. Ni and Fe in PB emulsions were extracted from crude oil with UV irradiation, which may provide an efficient process for metal removal. The emulsions were stable toward freeze/thaw cycles and their melting temperatures generally decreased with irradiation. Evidence of ·OH production existed when emulsions were exposed to UV but not to visible light. The presence of H₂O₂ enhanced the photodegradation of crude oil. Overall, the changes in emulsion properties were attributed to direct photodegradation and photooxidation of crude oil components.

1 Introduction

Crude oil is a complex mixture of hydrocarbons, organic compounds containing N, O, and S, and trace quantities of metals such as Ni, V, Fe, and Cu.^{1,2} One of the major sources of energy in the world, crude oil is continually being explored, processed, transported, stored, and utilized.³ However, oil spills can cause serious damage to the aquatic environment. Whether found at the bottom or on the surface of bodies of water, spilled oil is susceptible to physical, chemical, and biological weathering that cause its components to dissolve and disperse (emulsify) into the water column.^{4–7} Dispersants are surfactants and co-solvents that reduce the particle size and increase the surface area of crude oil components to facilitate physical, chemical, and biological degradation. Crude oil-in-water (O/W) emulsions consist of dispersed crude oil in the form of micelles in a continuous phase of water and have their own unique properties.⁸

The development of surfactant-based technologies associated with O/W emulsion will be useful in the remediation of oil spill and related environmental problems. These technologies, in connection with established methods to degrade crude oil, are promising new areas of study. Although there is high destruction of petroleum products in a marine environment,⁹ it is still crucial to investigate the characteristics and properties of crude oil emulsions in order to understand the disappearance of spilled crude oil in water through natural processes. For example, sunlight-mediated degradation of crude oil is a natural way of remediating crude oil pollution especially in tropical areas, in high seas where skimming would be impossible, and when chromophore-rich crude oil components are present.¹⁰ The use of TiO₂ promotes the photodegradation of crude oil components with air as an oxidant, but significant concentrations of Cl[–], SO₄^{2–}, and PO₄^{3–} ions in marine water have inhibitory effects as they compete with organic compounds for oxidizing sites on the TiO₂ surface.^{11,12} Additional cost, utilization of a very small UV region of solar radiation, and catalyst recovery make the use of TiO₂ infeasible on a large-scale basis.¹³

The development of novel photodegradation and surface-catalyzed oil degradation technologies depend on a more fundamental understanding of the photolytic degradation pathway. Photooxidation mechanisms include the reaction of crude oil components with active oxygen species and transformation of aromatic compounds into polar fractions (*i.e.*, hydroperoxides,

^aDepartment of Chemistry, University of Connecticut, 55 North Eagleville Rd., Storrs, CT 06269, USA. E-mail: steven.suib@uconn.edu; Fax: +1 860 486 2981; Tel: +1 860 486 2797

^bVeruTEK Technologies, Inc., 65 West Dudley Town Rd. Suite 100, Bloomfield, CT 06002, USA. E-mail: jcollins@verutek.com; Fax: +1 860 242 9899; Tel: +1 860 242 9800

† Electronic supplementary information (ESI) available: five figures and seven tables showing additional study details. See DOI: 10.1039/c2pp05275j

phenols, carboxylic acids, and ketones).^{14–16} Direct photodegradation instead of photooxidation has been observed in some studies.¹⁷ However, there are very few recent investigations that deal with photodegradation of crude oil or its components in natural water without the use of metal oxide catalysts and/or microorganisms. Due to the complexity of crude oil and the difficulties associated with extraction and fractionation of crude oil from water in an emulsion (e.g., cost, toxicity of organic solvents, and low resolution and percentage recovery),¹⁸ most work has been focused on direct photolysis of bulk crude oil and emulsions formed with very low water content.

Thus, we report here the preparation and characterization of crude oil emulsions, and the effects of visible and UV light irradiation on their properties. Synthetic seawater, plant-based surfactant, and Prudhoe Bay (PB) and South Louisiana (SL) crude oils were particularly chosen due to their environmental relevance. We demonstrate the changes in emulsion properties as key indicators of crude oil photodegradation. This study presents descriptive (phenomenological) treatability studies of crude oil in an emulsion using light, which will enable a better understanding for addressing an oil spill where coupled dispersion and photolytic destruction is applied.

2 Experimental

2.1 Preparation of emulsions

The US EPA reference Prudhoe Bay and South Louisiana crude oils were used. A novel, nonionic, and plant-based surfactant (VeruSOL®-Marine-200) was used as received.

The compositions of the surfactant before and after irradiation were also analyzed. Nuclear Magnetic Resonance (NMR) spectrometry and Direct Analysis in Real Time/Mass Spectrometry (DART/MS) experiments were conducted on a Bruker NMR instrument operating at 400 MHz and on a JEOL AccuTOF™/DART SVP spectrometer (with both DART and ESI ion source and a TOF/MS analyzer), respectively. For NMR analysis, the surfactant was dissolved first in MeOD and the same amount of CDCl₃ was added. For DART/MS, the atmospheric pressure interface conditions were: orifice 1 = 20 V, and both orifice 2 and ring lens were set to 5 V. The grid electrode voltage and gas temperature of the ion source used were +350 V and 350 °C, respectively. Fourier Transform Infrared (FTIR) analysis of the surfactant was conducted on a Nicolet 8700 FTIR spectrometer.

A 34.6 g L⁻¹ synthetic seawater was prepared by dissolving an appropriate amount of Instant Ocean® salt in ultrapure water (18.2 MΩ cm). Prudhoe Bay (PB) and South Louisiana (SL) emulsions were prepared from the crude oils, surfactant, and synthetic seawater. An emulsion was typically prepared by first mixing 1.0 g of surfactant with 1.0 L of synthetic seawater and then adding 5.0 g of crude oil in a 1.5 L cylindrical glass vessel. The surfactant to oil ratio was based on the critical micelle concentration of the surfactant and reflective to a proportion that would be used during application in contaminated surface water. The components were continuously mixed on an orbital shaker at 150 rpm for 72 h in the dark at ambient temperature. The concentrations of salt, surfactant, and crude oils were the same for all the emulsions prepared.

2.2 Visible and UV light irradiation of emulsions

Visible and UV light-emitting lamps were used to simulate components of natural solar radiation. Cool white (λ = mostly >350–700 nm, ~8 W) and black light (λ = 315–400 nm, ~90% in the 350 nm range, ~24 W) fluorescent lamps were used as constant, separate intense sources of visible and UV light, respectively. Sixteen lamps of each type were installed equally spaced on a Rayonet® Model RPR-100 photochemical chamber reactor. In a typical experiment, a 200 mL quartz cylindrical vessel containing 50.0 mL emulsion sample was placed on a magnetic stirrer at the center of the photoreactor (~10 cm away from the lamps) and remained closed during irradiation.¹⁹ Prior to irradiation, the emulsion was saturated with UHP-grade air for 30 min with continuous stirring. The concentration of dissolved oxygen in emulsion was measured using a YSI Model 550A DO meter. UHP-grade argon gas was used for experiments that exclude dissolved oxygen. Visible and UV light irradiation of emulsions were conducted in a batch-type reaction for three trials with continuous stirring. The operating temperatures inside the photoreactor utilizing visible and UV lamps were approximately 29 and 35 °C, respectively, held fairly constant by a cooling fan. Synthetic seawater and surfactant in seawater blank solutions, and emulsions containing 1% H₂O₂ were also analyzed according to the procedure described above.

2.3 Characterization of emulsions

A McCrone Olympus Model BX50 optical microscope was used to observe the dispersed crude oil in emulsions. Direct observation of emulsions in their natural state was also carried out using an FEI ElectroScan 2020 Environmental Scanning Electron Microscope (ESEM) without further dilution or sample preparation. The ESEM was equipped with a tungsten filament, a Peltier-controlled cooling stage, a backscattered electron detector, and a gaseous secondary electron detector. The accelerating voltage was set at 20.0 kV. Samples were cooled to temperatures between 7.0–9.0 °C and maintained at a pressure of 5.0 Torr to achieve a saturated vapor pressure of water. A 0.1 mL sample of each emulsion was placed in the specimen chamber. Due to fluid mobility, scanning was done at high rates to allow better resolution of images.

Dynamic Light Scattering (DLS) experiments were performed using a Malvern Zetasizer Nano ZS90 instrument equipped with a 4 mW He–Ne ion laser (λ = 633 nm) at a measurement angle of 90°. The hydrodynamic size as Z-average diameter of crude oil micelles and their size distribution in emulsions were determined. The zeta (ζ) potentials of emulsions were also measured to assess emulsion stability. All DLS measurements were performed at 25.0 °C without sample dilution.

The change in the concentrations of Ni, V, and Fe as a function of irradiation time, and the initial concentrations of Mg, K, and Na in the water phase of emulsions were determined using a Thermo Jarrell Ash model ICAP 61E trace analyzer Inductively-Coupled Plasma/Atomic Emission Spectrometer (ICP/AES). A demountable center tube quartz plasma torch was used. A built-in peristaltic pump was used to feed the nebulizer with the sample solution. Argon gas was utilized. Standard solutions for calibration for V, Mg, K, and Na were prepared from their stock

salt solutions. Standard solutions for Fe and Ni were prepared from their metallic forms by dissolving appropriate amounts of these metals in a HNO_3 -HCl mixture. The wavelength lines used were 231.604 nm (Ni), 292.402 nm (V), 271.441 nm (Fe), 279.079 nm (Mg), 766.491 nm (K), and 330.237 nm (Na). The samples were diluted 8× with ultrapure water. The concentrations of Cl^- and SO_4^{2-} ions in emulsions were determined using potentiometric titration and spectrophotometric method, respectively. All reagents used were of highest purity and all glassware used was acid-washed prior to use.

Differential Scanning Calorimetric (DSC) technique was used to determine the crystallization and melting temperatures of emulsions before and after irradiation. Analyses were conducted on a Thermal Analysis DSC Q100 instrument which was continuously flushed with nitrogen at a flow rate of 50 mL min^{-1} . A hermetically-sealed aluminum pan with lid was used as a sample container. The mass of the sample ranged from 10–20 mg. An empty pan was used as a reference. Typically, the emulsion sample was first heated to 30 °C. The sample was then cooled by using liquid nitrogen down to –60 °C, keeping at this temperature for 3 min, and then reheating the sample again to 30 °C (first cycle). The second cycle was performed to analyze the influence of the first cycle regarding the stability of the samples and to corroborate the position of the peak. Heating and cooling rates were set at 1 °C min^{-1} .

The bulk physical properties of emulsions were characterized further. Freshly prepared emulsions were also used in every analysis. The temperature, pH, and conductivity of emulsions were measured using an Oakton pH 510 Series pH/mV/°C meter. The viscosity and density of emulsions were measured using an Ostwald viscometer and a pycnometer, respectively.

The UV fluorescence (UVF) spectra of emulsions were collected on an Agilent Cary Eclipse fluorescence spectrophotometer using a 1.0 cm quartz cuvette at ambient temperature. For synchronous scanning, excitation and emission monochromators were offset by 20 nm. Emissions between 280 and 480 nm were recorded and 2.5 nm slit widths were used. UVF spectrophotometric technique was used to monitor the extent of photodegradation and photochemical behavior of crude oils in emulsions and to indirectly detect hydroxyl radicals (·OH) using terephthalic acid as an indicator.¹⁹

The ability of visible and UV light to remediate crude oil-contaminated water in the presence of surfactant was investigated by measuring the concentrations of Total Petroleum Hydrocarbons Gasoline Range Organic (TPH-GRO) and Diesel Range Organics (TPH-DRO) in emulsions before and after irradiation following the US EPA Method 8015. Analyses of the Volatile Organic Compounds (VOCs) and the Semi-Volatile Organic Compounds (SVOCs) in emulsions were also performed following the US EPA Methods 8260C and 8270, respectively.

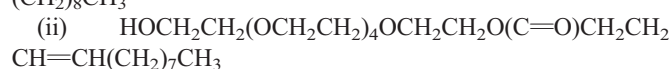
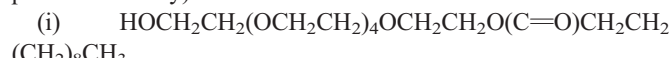
3 Results and discussion

3.1 Compositions of emulsions

The DART/MS signatures of the PB and SL crude oils showed the presence of several clusters (Fig. S1†). This result indicates the complexity of the crude oil samples similarly observed in a

recent work.²⁰ Other important properties of the crude oils were also reported (Table S1†).

VeruSOL®-Marine-200 surfactant is a light yellow, odorless, water-soluble, and nearly neutral ($\text{pH} = 7.4$) liquid. This surfactant contains no solvents or petroleum products and is made of a single non-ionic, plant oil-based surfactant. Performance results indicate excellent emulsification of the SL crude oil once the critical micelle concentration is achieved. NMR analyses of the surfactant showed four major components in solution (Table S2†): (i) ~65% was straight chain fatty acid attached to a hexamer of ethylene glycol, $\text{C}_{25}\text{H}_{48}\text{O}_8$; (ii) ~30% has a *cis*-alkene within the fatty acid and was attached to the hexamer of ethylene glycol, $\text{C}_{25}\text{H}_{48}\text{O}_8$; (iii) a small amount (~5%) of propan-2-ol; and (iv) a sugar (α and β glucose by virtue of the coupling constants and overlapping signals, shifted by solvent pH and viscosity):



DART/MS analysis of the surfactant confirmed the presence of ethoxy repeating units (Fig. S2†).

The ions present in synthetic seawater solution in appreciable amounts were Na^+ (18720 mg L^{-1}), Cl^- (9560 mg L^{-1}), SO_4^{2-} (1875 mg L^{-1}), Mg^{2+} (1047 mg L^{-1}), K^+ (1037 mg L^{-1}), and Ca^{2+} (515 mg L^{-1}).

3.2 Characteristics and properties of emulsions

3.2.1 Appearance and color. The physical and chemical properties of emulsions were characterized before and after irradiation to gain a better understanding of crude oil degradation. PB and SL crude oils formed emulsions in water with tints of clear yellowish-brown and clear reddish-brown colors, respectively (Fig. 1, inset). A drop of each emulsion spontaneously dispersed in water in a dilution test. A change of color from red to green was observed when methyl orange indicator was mixed with each emulsion. Under the optical microscope, both emulsions showed dispersed crude oil of uniform shape but different sizes in the continuous water phase (Fig. 1). Results of dilution and indicator tests, and optical and electron microscopy studies imply that crude oil and water are the dispersed and

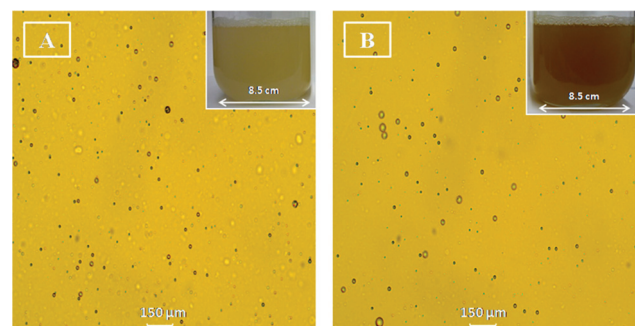


Fig. 1 Representative optical micrographs of the (A) Prudhoe Bay and the (B) South Louisiana crude oil-in-water emulsions before irradiation. Tiny crude oil particles are dispersed in the continuous phase of water. Insets show the photographs of freshly prepared emulsions.

continuous phases, respectively. The crude oil particles were mobile; hence, it was difficult to image and estimate their sizes at high magnifications. A detailed study of the appearance and structure of crude oil was therefore conducted. ESEM allowed direct visualization of O/W emulsions in the hydrated state.^{21,22} Crude oil (higher intensity image) was dispersed in a continuous phase of water (lower intensity image) as micelles and had components on the water surface (Fig. 2A–L). The observed bright numerous specks/areas against the dark water phase were part of the crude oil. Images of crude oil micelles were more clearly observed in SL emulsions at high magnifications. The size of micelles ranged from a few hundred nanometers to \sim 10–15 μm . On the surface were some crude oil micelles and oil components floating, which were prominent in PB emulsions. These crude oil components are presumably those which did not or were difficult to emulsify in surfactant–water mixtures. Images also showed irregularly-shaped crude oil components spread on the surface containing some \sim 20–30 μm -sized water components (Fig. 2C–F). However, after UV light irradiation, images of crude oil micelles were difficult to visualize (Fig. 3).

ESEM technique has been used for investigating the behavior of large numbers of emulsions and their properties.^{21–24} The observed contrast in the ESEM images of emulsions before irradiation is attributed to variations in the secondary electron emission characteristics arising from the difference in electronic

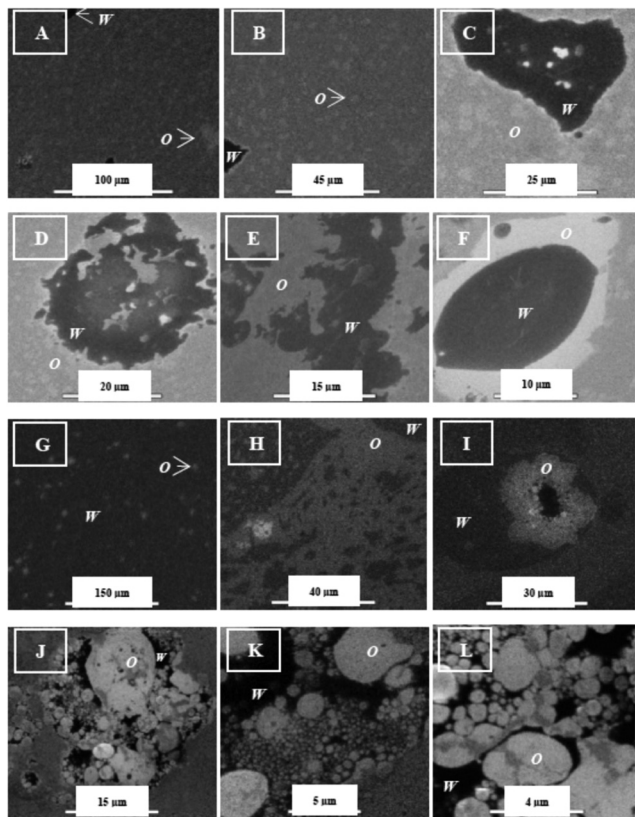


Fig. 2 Representative ESEM images of the (A–F) Prudhoe Bay and the (G–L) South Louisiana crude oil (*O*)-in-water (*W*) emulsions before irradiation. Crude oil components (higher intensity) are present both on the water surface and dispersed as micelles in the continuous phase of water (lower intensity).

properties^{22,23} between crude oil components and water. Two key factors significantly determine the variation of contrast in the images in this study; the generation of secondary electrons within the sample and the transport of secondary electrons through the sample.²² The secondary electrons generated within the sample are mainly contributed by the presence of relatively high atomic number elements²² such as Ni, V, and Fe present in both crude oils. The lighter contrasts in the images can be attributed to high concentrations of these metals in those regions. Secondary electrons will be generated in the same manner should the emulsions contain only relatively low atomic number elements including H, C, N, O, and S. For example, no image contrasts were observed for the surfactant in water, thus, there were no significant secondary electron emission effect contributions from the surfactant alone. This could also be due to the relatively low concentration of the surfactant used. Kinetic energy is lost when secondary electrons diffuse through the sample and the extent of this diffusion depends on the dielectric properties of the substances.²² This factor also determines the image contrasts. Water and the hydrocarbon components of crude oils have different dielectric responses contributed by the individual bonds contained in these molecules.

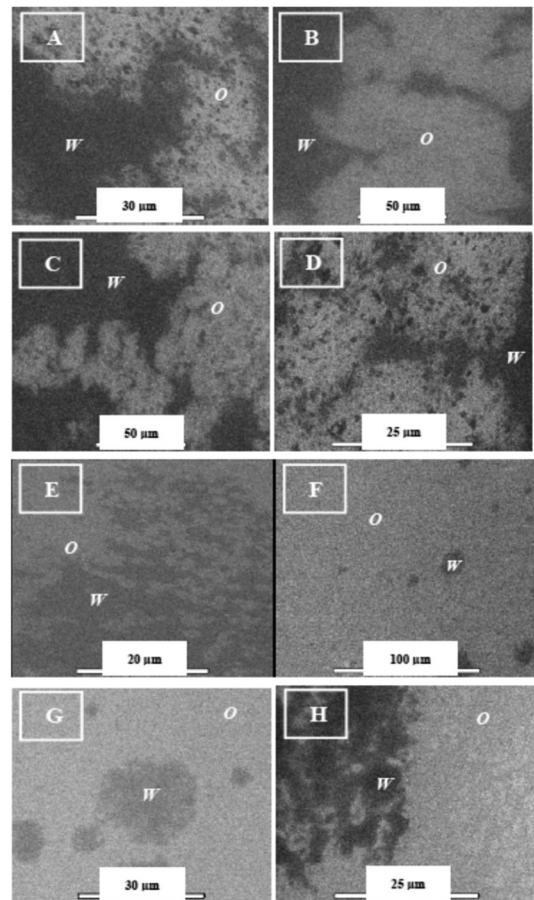


Fig. 3 Representative ESEM images of the South Louisiana crude oil (*O*)-in-water (*W*) emulsions at different magnifications after (A–B) 30 min, (C–D) 60 min, (E–F) 90 min, and (G–H) 120 min of UV irradiation.

3.2.2 Crude oil micelles size and distribution. The Z-average diameter of surfactant micelles before the addition of crude oil was 0.135 μm . Following the addition of crude oil under dark conditions, the Z-average diameter of micelles in SL emulsions was in a range of 0.64–0.69 μm , $\sim 3\times$ larger than those in PB emulsion (0.23–0.24 μm). Clearly, crude oil micellarization resulted in a swelling of micelles. The Z-average diameter of crude oil micelles generally and gradually decreased with increasing exposure to visible and UV light (Fig. 4). Upon UV irradiation for 120 min, a 58% size reduction was found for the PB emulsion and a 47% reduction for the SL emulsion, resulting to a micelle size close to that of the surfactant alone. Using visible light for 120 min, the micelle size was reduced by only 19% and 32% for PB and SL emulsions, respectively. Much smaller micelles (~ 10 nm–1 μm) were also formed.

Proof of the polydispersity initially observed in the ESEM images was also obtained using DLS experiments. A high degree of polydispersity of crude oil micelles was observed before and after irradiation (Fig. 5). Dispersed crude oil particles had a propensity to form extremely small micelles (<100 nm) with increasing irradiation time.

The size and distribution of the dispersed phase particles are critical in determining the stability and properties of emulsions.²⁵ The sedimentation rate of crude oil micelles is faster when the size and density differences between phases are increased.²⁵ Since the micelle size is found to generally decrease with irradiation, coalescence of small crude oil micelles into larger ones may not be a plausible explanation for the decreasing trend in stability of emulsions. Small micelle size imparts stability if the crude oil micelles are electrostatically or sterically interacting.^{8,25} A small volume of the dispersed phase reduces the frequency of collisions and aggregation.²⁵ If the emulsions generally form smaller crude oil micelles with irradiation, and yet results show that stability decreases, then photodegradation of crude oil components is the major factor in decreasing stability of emulsions. Nevertheless, with the proportions of small and large micelles markedly different, any change in particle size distribution following irradiation is an indication of the extent of photodegradation and the strength of emulsions prepared. The formation of smaller micelles is crucial for enhancing

the rate of crude oil photodegradation in emulsions, which can occur due to their high surface areas.⁸

3.2.3 Stability. Highly negative ζ potential values were obtained for emulsions. Dispersed crude oil micelles acquired a negative surface charge in aqueous solutions having salt concentrations and pH values measured in this study. The ζ potential value of the surfactant mixture without crude oil was -65.9 mV. When crude oil was added, the ζ potential values became more negative indicating formation of more stable emulsions (Fig. 6), despite observation in the ESEM that some oil components were floating. The emulsions irradiated with UV became relatively less stable than the emulsions irradiated with visible light.

Repulsive forces such as electrostatic and steric repulsions cause stabilization of emulsions. Surfactants stabilize the emulsions by increasing the strength of the interfacial film between the crude oil phase and water phase.²⁶ Nonionic surfactants have the advantage of insensitivity to the salt content of the water phase^{27,28} and have a positive contribution in forming stable, low viscosity O/W emulsions.^{8,29} Here, the surfactant used has a major component that resembles an alcohol ethoxylate-type nonionic surfactant. According to the steric stabilization theory, nonionic surfactants stabilize the crude oil dispersed phase by repulsive interactions.³⁰ These steric repulsions can occur between the hydrated hydrophobic tail of the nonionic surfactant

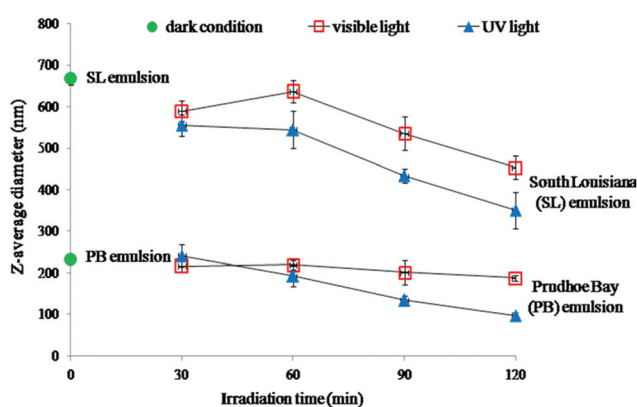


Fig. 4 Average ($n = 3$) Z-average diameter size of crude oil micelles in Prudhoe Bay (PB) and South Louisiana (SL) emulsions as a function of irradiation time. Error bars are at the 95% confidence intervals.

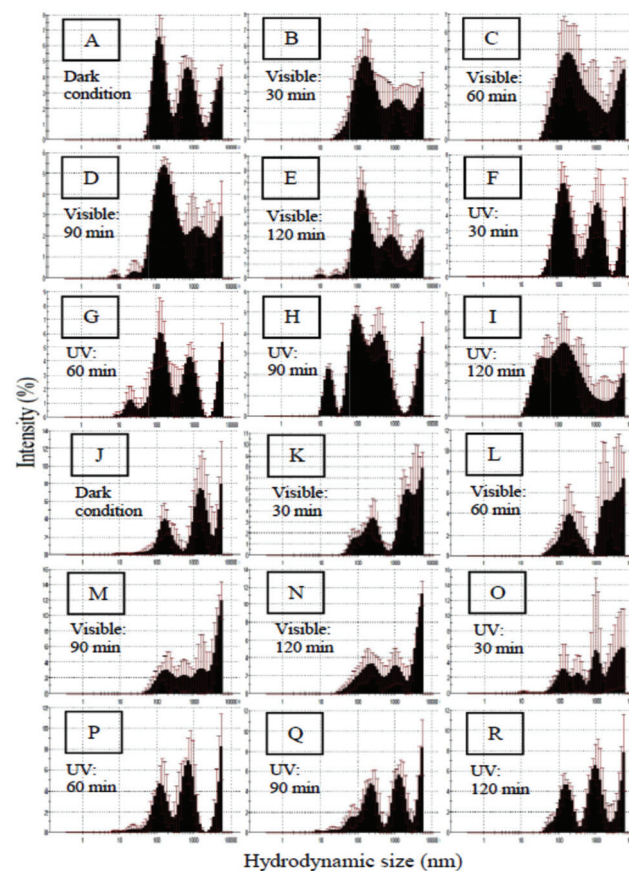


Fig. 5 Intensity time-averaged light scattering (%) as crude oil micelle size distributions in the (A–I) Prudhoe Bay and the (J–R) South Louisiana emulsions before and after visible and UV light irradiation.

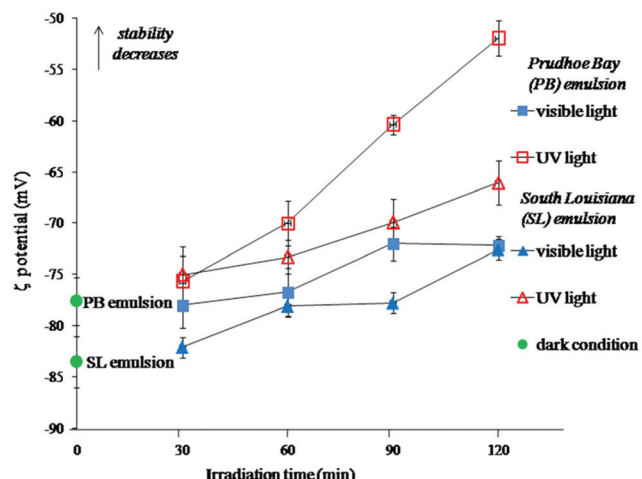


Fig. 6 Average ($n = 3$) zeta (ζ) potentials of the Prudhoe Bay (PB) and the South Louisiana (SL) emulsions as a function of irradiation time. Error bars were at the 95% confidence intervals.

adsorbed at the surface of the dispersed crude oil micelles and the neighboring micelles. These repulsions thus help prevent coalescence. An increase in the number of polyethylene glycol chains in the nonionic surfactant increases their solubility in water, decreases their sensitivities to pH changes, and enhances sample transport processes.^{28,31} This could be crucial for the biodegradability of emulsions. The surfactant used also contains some degree of unsaturation in its structure. The presence of a *cis* double bond in the surfactant can cause the chain to bend and impart considerable bulkiness that is favorable with respect to geometrical packing properties. Interestingly, this double bond can also act as a π -electron donor to form a complex with powerful acceptor molecules such as aromatics with electron-withdrawing substituents abundant in crude oils.³² Structure plays a vital part in the interaction between surfactants and the oil phase. The presence of natural surfactants in crude oil is critical to emulsion stability.^{33,34} The acidic components of crude oil are more effective in stabilizing emulsions when they are not ionized. The negative ζ potential charge of emulsions is caused by the interfacially active components of crude oil. When light is introduced, the percentage of absorption is then reduced which leads to a decreasing number of negative charges on the crude oil micelles, thus, reducing the absolute value of ζ potential (destabilized emulsion). Likewise, the velocity of micelles in the electric field is decelerated which results in a similar reduction in the magnitude of ζ potential.³⁵

3.2.4 Concentration of metals. After 120 min UV irradiation, the concentration of Ni in the aqueous phase of PB emulsion increased by over 100% (Fig. 7). The concentration of Fe increased by 77% under the same conditions and also generally increased when subjected to visible light. This trend was observed in SL emulsion only when irradiated with UV from 60 to 120 min. No experimental evidence was found to support possible conversion of metal porphyrin compounds to metal oxides in crude oil emulsions by photochemical activation. Good agreement between results using ultrapure water and

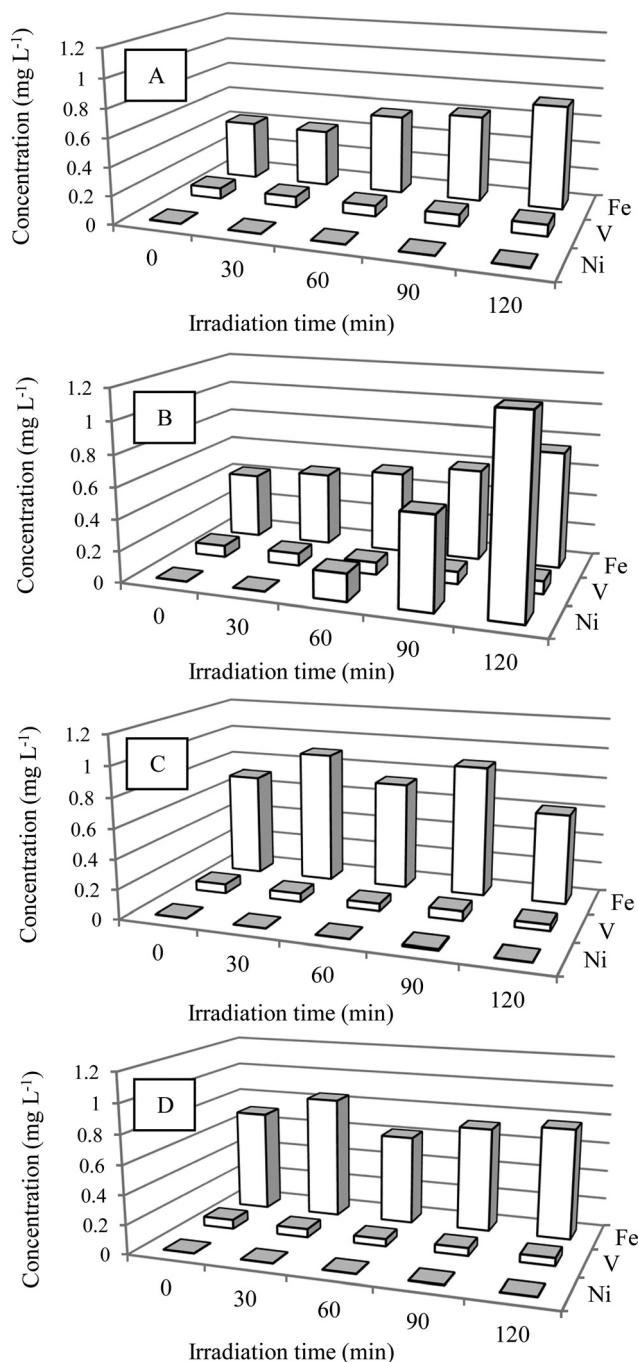


Fig. 7 Average ($n = 3$) concentrations of heavy metals (Ni, V, and Fe) in the aqueous phase of the Prudhoe Bay emulsions [(A) visible and (B) UV light irradiated] and of the South Louisiana emulsions [(C) visible and (D) UV light irradiated]. Multi-element standard solutions for calibration were prepared using ultrapure water and blank solution. External standard calibration was used to calculate the concentrations from emission intensities.

surfactant solutions as calibration standards validates the absence of effects of interfering species.

Metals in crude oil exist as complex organometallic complexes in the form of porphyrins, nonporphyrin metallic chelates, colloidal suspensions, and/or metallic soap.^{1,36} Ni and V were found, but the presence of Fe in crude oils could be due to the

existence of Fe porphyrins or contributed by corrosion products collected during transportation. The increase in concentration of metals in the water phase of emulsions implies that metals come out of crude oil with light treatment. This can be an effective, novel way to clean up oil contaminated water and may provide an efficient process for metal removal in crude oils. Removal of metal is significant since such metals can destroy fluid cracking catalysts and change the distribution in the gasoline fraction. No significant change in the concentration of V was observed after irradiation, which could be due to the presence of sulfur in crude oils which acts as a retaining agent.³⁷ The successful analysis of metals in the water phase of emulsion with a high degree of precision suggests homogeneity of the samples.³⁶

3.2.5 Thermal properties. Thermal analysis provides a way of studying emulsions that evolve with irradiation. The crystallization and melting temperatures of emulsions from the first cycle were consistent with the second cycle suggesting emulsion stability toward freeze/thaw cycles.¹⁸ The crystallization temperatures of non-irradiated PB and SL emulsions were $-7.3\text{ }^{\circ}\text{C}$ and $-8.0\text{ }^{\circ}\text{C}$, respectively. There was a direct correlation between the Z-average diameter size of crude oil micelles of irradiated emulsions and their crystallization temperatures (Fig. 8). As the micelle particle size becomes smaller, the crystallization temperature becomes lower. In general, a longer irradiation time resulted in lower crystallization temperatures. A previous study on oil emulsions has shown that crystallization temperature is composition dependent.¹⁸ The melting temperatures of non-irradiated PB and SL emulsions were $3.4\text{ }^{\circ}\text{C}$ and $5.9\text{ }^{\circ}\text{C}$, respectively. No general trend was observed for melting temperature as a function of micelles size and irradiation time in both emulsions.

3.2.6 Other bulk physical properties. Measurements of bulk physical properties of emulsions were conducted (Table 1). The pH values of irradiated emulsions were consistently more acidic than the pH values of emulsions under dark conditions. Substantial decreases in the average pH values were observed for both emulsions as a function of irradiation time. For example, the pH values of PB and SL emulsions were lowered by as much as

1.45 and 0.11 units after exposure to UV light for 120 min. The same reduction in pH values (0.49) was observed for both emulsions treated with visible light for 120 min. There was no significant change in the pH of the surfactant in seawater with increasing irradiation time. In PB emulsion after 30 min UV irradiation, the concentrations of oleic acid, tetradecanoic acid, and n-hexadecanoic acid increased, and formation of

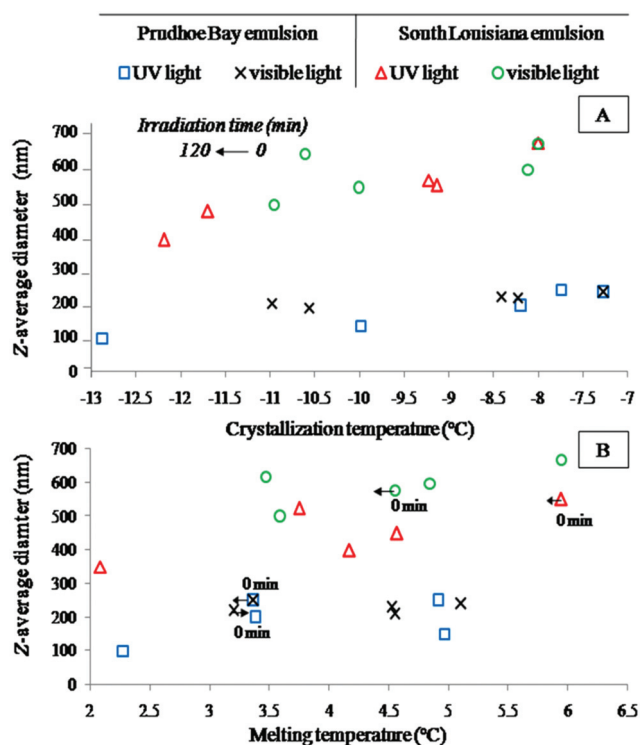


Fig. 8 Correlation between the Z-average diameter size of crude oil micelles in the Prudhoe Bay (PB) and the South Louisiana (SL) emulsions irradiated with visible and UV light and their (A) crystallization and (B) melting temperatures for which the intensity of the DSC curve is maximized. Direction of the arrows indicates the general trend of how crystallization and melting temperatures vary with irradiation time.

Table 1 Some bulk physical properties of the Prudhoe Bay (PB) and the South Louisiana (SL) emulsions before and after irradiation^a

Sample	pH		Conductivity (mS cm ⁻¹)		Density (g mL ⁻¹)		Viscosity (cP)	
Seawater	7.70		51.2		1.0212		0.9238	
Surfactant in water	7.73		51.9		1.0212		0.90571	
<i>Treatment</i>	<i>PB emulsion</i>	<i>SL emulsion</i>	<i>PB emulsion</i>	<i>SL emulsion</i>	<i>PB emulsion</i>	<i>SL emulsion</i>	<i>PB emulsion</i>	<i>SL emulsion</i>
Dark conditions	7.15	6.90	0.422	0.433	0.9977	0.9975	0.8859	0.8803
Visible light								
30 min	6.74	6.68	0.471	0.459	0.9972	0.9976	0.8757	0.8782
60 min	6.77	6.72	0.502	0.507	0.9973	0.9977	0.8736	0.8775
90 min	6.68	6.62	0.609	0.556	0.9975	0.9977	0.8746	0.8788
120 min	6.66	6.41	0.638	0.634	0.9977	1.0029	0.8733	0.8950
UV light								
30 min	6.79	6.80	0.481	0.456	0.99734	0.99809	0.8762	0.8949
60 min	6.31	6.72	0.509	0.491	0.99799	0.99706	0.8786	0.8980
90 min	6.20	6.77	0.555	0.524	0.99794	0.99748	0.8851	0.9101
120 min	5.70	6.79	0.582	0.540	0.99777	0.99780	0.8883	0.9157

^a Data reported are the average of three trials.

3-hydroxypropyl ester oleic acid was observed (Table S3†). In SL emulsion, 9-hexadecenoic acid ($3900 \mu\text{g L}^{-1}$) and dodecanoic acid ($3700 \mu\text{g L}^{-1}$) were formed after 30 min UV irradiation, whereas 9-octadecenoic acid (*Z*)-2-hydroxy ($30\,000 \mu\text{g L}^{-1}$) and oleic acid ($79\,000 \mu\text{g L}^{-1}$) were identified after visible light irradiation (Table S4†). The increase in concentration and the formation of carboxylic and fatty acids could explain the drop in pH values in PB emulsions with irradiation. The difference in pH change between the two emulsions could be explained by the difference in the compositions of the two crude oils. Free radical oxidation of substituted polycyclic aromatic hydrocarbons (PAHs) and/or breakdown of long chain acids in crude oil could have resulted in an increase in concentration and production of acid molecules. Acidification may have consequences for pH sensitive organisms.

The addition of surfactant slightly increased the conductivity of seawater. However, a $>90\%$ reduction in conductivity was observed in the presence of crude oil. In general, continuous UV irradiation increased the conductivities of emulsions slightly more than visible light irradiation. The densities of emulsions were less than the density of synthetic seawater with or without the surfactant. There was no significant difference between the densities of emulsions before and after irradiation. The viscosities of crude oil samples decreased when they were emulsified in seawater in a form of the O/W type. The presence of surfactant and crude oil lowered the viscosity of seawater by only $\sim 4\%$. Longer irradiation time resulted in increased viscosities of both crude oil emulsions. The conductivity of emulsions increases as a result of formation of ionized compounds upon irradiation. This is due to a release of ionic species that are soluble in the continuous water phase. Dissolved hydrated ions become smaller when a surfactant is added in pure water.³⁰ This explains the slight increase in the equivalent conductivity of seawater when surfactant was added. Enhanced degradation could then easily take place if crude oil components are converted to more water-soluble compounds, which are simply transported in water.

Industrially, O/W emulsions are made to reduce the viscosity of crude oils and bitumens so that they can be effectively transported through pipelines²⁷ and are important for preventing corrosion and formation of sediments in pipes.³⁸ The increase in viscosity of emulsions when irradiated can be explained by unavoidable evaporative loss of volatile contents of crude oil. Formation of smaller crude oil micelles during irradiation not only has physical significance in terms of stability but also has effects on viscosity. Smaller micelles promote viscous emulsions due to more particle-particle interactions as a result of a larger interfacial area.³⁸ However, relatively larger micelles result in unstable emulsions with lower viscosity.³⁹

3.2.7 Fluorescence characteristics. Fig. 9 shows the representative fluorescence spectra of emulsions before and after irradiation. Both non-irradiated emulsions showed broad emission spectra in the 340–420 nm wavelength regions. In PB emulsions, the maximum fluorescence signal was reduced by 67% with visible light and 90% with UV light after 120 min. In SL emulsions, the reductions were 50% and 90% with visible and UV light irradiation, respectively. A small fluorescence peak at 425 nm was common in all spectra and attributed to a signal

from the surfactant. Based on the relative fluorescence intensities, the surfactant did not seem to degrade upon irradiation even with the addition of 1% H_2O_2 (Fig. S3†). NMR, DART/MS (Fig. S4†), and FTIR (Fig. S5†) analyses further revealed that the surfactant did not degrade with irradiation.

Irradiation of emulsions in the presence of 1% H_2O_2 , however, significantly lowered their TPH-DRO and TPH-GRO concentrations (Table S5†). Seawater blank solution did not show any fluorescence peaks. In dark conditions, the corresponding emulsions that were treated in exactly the same way showed no significant alterations in fluorescence intensities. The synchronous fluorescence spectra of irradiated PB and SL emulsions also show a progressive decrease in the spectral intensity with irradiation time (Fig. 10). This effect was similarly observed in previous studies.^{32,40,41} More fine structures are apparent using the synchronous scanning mode, indicative of the complex mixture of fluorescing aromatic compounds present in emulsions.

When subjected to irradiation, light absorption by crude oil emulsions is possible in the presence of conjugated PAHs, the more reactive components of crude oil.¹⁰ Emissions in the 265–385 nm region indicate the presence of 1,4-fused aromatic rings.⁴² Similar to these observed results, maximum emissions in

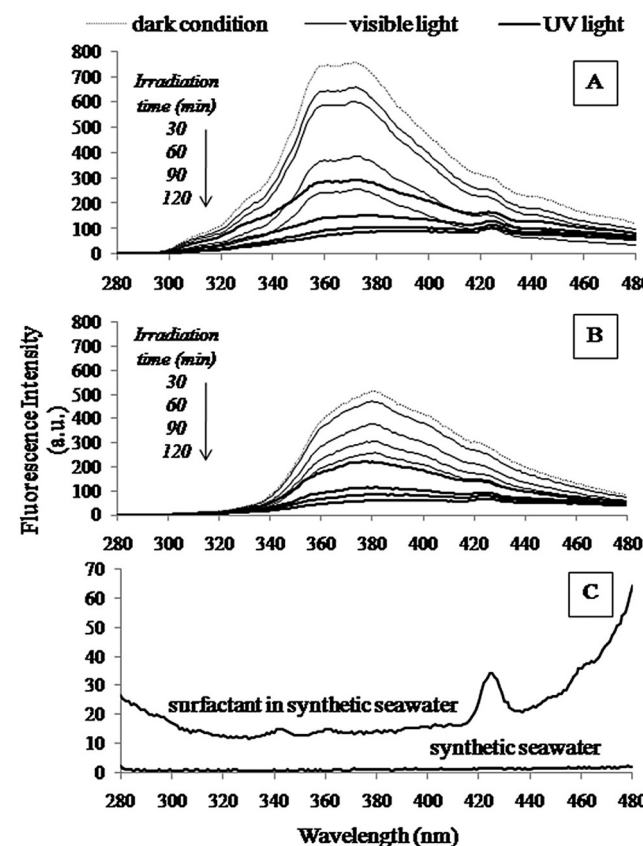


Fig. 9 Fluorescence emission spectra of the (A) Prudhoe Bay and the (B) South Louisiana emulsions as a function of visible and UV irradiation time, and of the (C) synthetic seawater and non-irradiated surfactant. Fluorescence intensities are the average of three replicate measurements. Excitation wavelengths were set at 250 nm. Excitation and emission slit widths were set at 5 nm.

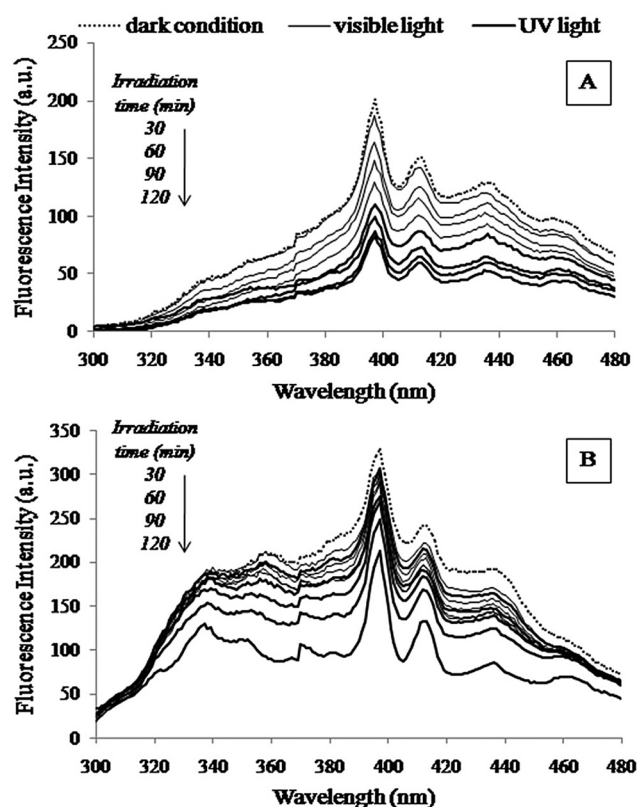


Fig. 10 Synchronous fluorescence spectra of the (A) Prudhoe Bay and the (B) South Louisiana emulsions as a function of visible and UV irradiation time. Fluorescence intensities are the average of three replicate measurements.

the 296–310 nm and in the 320–330 nm regions both indicate the presence of aromatic hydrocarbons in crude oils.⁴² The polynuclear aromatics absorb strongly in the near UV region (>290 nm). Marked decreases in the concentrations of naphthalene, 1-methylnaphthalene, 2-methylnaphthalene, and phenanthrene, and in the concentrations of the majority of VOCs and SVOCs in emulsions before and after irradiation were observed (Tables S3–S4 and Tables S6–S7†). This could explain the observed decreasing fluorescence in emulsions as a function of irradiation time. Light can generate reactive species that can oxidize the low molecular weight, water-soluble fraction of crude oil which affects the fluorescence of emulsions.^{16,43}

Photodegradation leads to loss of fluorescence emission in the far UV range. The different responses to various irradiation wavelengths could also be due to variations in the compositions of crude oils. For example, aromatic hydrocarbons initially present in emulsions could react with light to yield non-fluorescent compounds.⁶ The formation of polar groups such as carbonyl groups accompanies an increase in the water-soluble extractable components which are poorly-fluorescing. Some are degradation products not originally present in crude oil. The portion of the solar spectrum responsible for photodegradation is primarily the UV region with 95% UV-A (~315–400 nm).⁹ The decrease in fluorescence emission using visible light could be due to direct photolysis of visible light-absorbing chromophores in crude oils when present in emulsions.

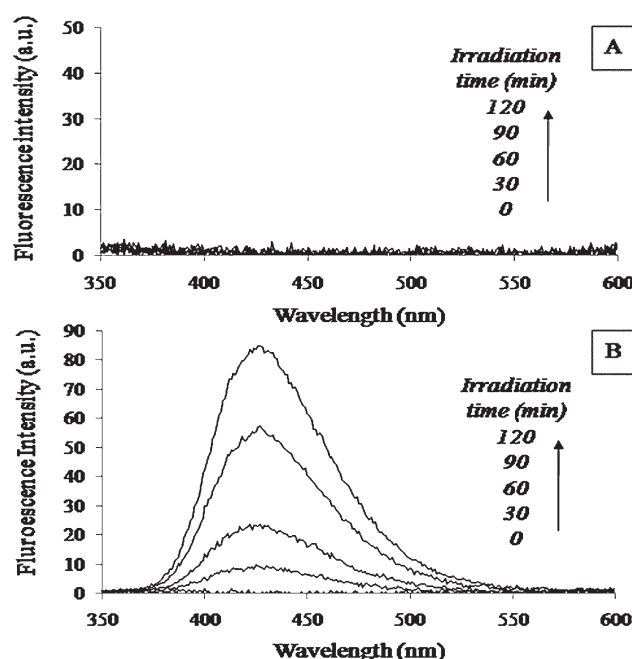


Fig. 11 Fluorescence emission spectra of the surfactant containing 0.10 M terephthalic acid solution (indicator) under air saturation (average dissolved O_2 concentration at 0 min is $\sim 8.0 \text{ mg L}^{-1}$) after (A) visible and (B) UV light irradiation. Excitation wavelengths were set at 320 nm. Excitation and emission slit widths were set at 5 nm. Data reported are the average of three replicate measurements.

Terephthalic acid produced the fluorescent product, monohydroxyterephthalate, from its reaction with photogenerated $\cdot OH$.¹⁹ Emulsions treated with visible light did not produce any significant fluorescent product (Fig. 11). With UV irradiation, however, the emissions in the visible range appeared as strong and broad peaks with maxima at 427 nm. The fluorescence intensities of emulsions treated with UV light increased with irradiation time. Aside from acidic compounds, a variety of oxygenated hydrocarbons (*i.e.* VOCs) were produced after irradiation. In PB emulsions, acetone, carbon disulfide, alkylated benzenes, alkylated cyclohexanes, hexylpentyl ether, trichlorooctadecylsilane, tridecane, and nonanal were formed. In SL emulsions, chloromethane, 2-butanone, carbon disulfide, dichloroethene, alkylbenzenes, substituted decanes, hexanal, heptanal, and octanal were formed.

Photooxidation of organic compounds involves the action of a reactive oxidant including $\cdot OH$.^{16,17} Free radical-based oxidation by photochemical reactions can act on crude oil components in water with dissolved hydrocarbons as well as with dispersed crude oil emulsions.⁹ Dissolved O_2 contributed to the creation of $\cdot OH$ since the emulsions did not give any fluorescence signal when saturated with argon gas. The free $\cdot OH$ react with free organic molecules in the bulk of the emulsion, a known reaction causing H-abstraction from the hydrocarbons.⁴³ At pH 7.0, addition of CH_3OH , an $\cdot OH$ scavenger, decreased the rate of degradation. This suggests that the reaction occurred mainly in the bulk solution, where $\cdot OH$ were effectively scavenged by the CH_3OH molecules. Emissions in the visible spectrum range increase as $\cdot OH$ species are produced with continuous UV

irradiation and higher photooxidation is thus observed. As UV light is attenuated through the water phase, the presence of $\cdot\text{OH}$ is important in the oxidation of organic components of crude oil in emulsions.

The addition of H_2O_2 enables chemical oxidation to take place either by mineralizing dispersed crude oil constituents or by transforming them into more degradable compounds. Additionally, H_2O_2 enhances photooxidation reactions with UV wavelengths in the natural sunlight spectra, and significantly stimulating aerobic biodegradation of the dispersed crude oil; the result of the production of O_2 associated with the decomposition of peroxide.¹⁶ In water, it is well-documented that peroxide can produce photo-Fenton reactions. It is also known that micellarization of crude oil constituents, such as PAHs, leads to faster rates of aerobic microbial degradation and photodegradation.¹⁶ In open water, estuarine, and sediment environments where hypoxia already exists or is close to occurring (for example, in the Gulf of Mexico region), the addition of H_2O_2 can help offset hypoxia due to the significant increase in crude oil-related substrates (with or without added flux of crude oil substrates associated with the use of dispersants alone) entering these environments.

4 Conclusions

Crude oil-in-water emulsions have been successfully prepared using synthetic seawater, hydrophilic nonionic surfactant (VeruSOL®-Marine-200), and Prudhoe Bay and South Louisiana crude oil samples. The properties of emulsions have been carefully characterized providing a basis for further work relating to oil-dispersant emulsion formation and efficiency in oil spill dispersant design.

Contrast differences between the aqueous phase and the crude oil phase in the ESEM images are sufficient to study the structure of these emulsions. ESEM techniques can be used for distinguishing hydrocarbons with different degrees of saturation and for studying the extent of crude oil photodegradation. Measurement of emulsion properties including stability, crude oil droplet size and distribution, density, viscosity, pH, and conductivity has proven to be a general strategy in studying the chemistry of emulsions. Trace metal analysis helps assess homogeneity of emulsions and monitor changes in metal concentrations with irradiation time. Thermal analyses show a relationship between freezing temperature and change in droplet size. Due to compositional complexity of the emulsions, the effects of visible and UV light irradiation on these properties have been used as indirect indicators for photodegradation. The unique changes in various properties have provided a clear explanation and a novel way of assessing crude oil degradation and emulsion stability. Stability measurements used here can be applied for further development of emulsion breakers, recyclability of surfactants, and inhibitor testing for environmental applications.

Significant findings concerning the role of visible and UV light on the degradation of crude oil in O/W-type emulsions have been presented. Photodegradation stimulates degradation of crude oil components through reaction with $\cdot\text{OH}$. Photodegradation of crude oil components can be an effective process for

mitigating some of the damaging impacts resulting from oil spills in the aquatic environment. Much more water-soluble photoproducts should therefore be more easily transported to and taken up by the aqueous organisms. There could be enhanced bioavailability enabling further degradation of crude oil components and their photoproducts following exposure to sunlight. Future work may focus on enhancing biodegradability and studying the effects of photoproducts in the natural environment (e.g., phototoxicity). Modern efficient UV-visible light sources may enable economic application of photodetoxification on a large-scale basis.

Acknowledgements

This work was supported by VeruTEK Technologies, Inc. and the U.S. Department of Energy, Office of Basic Energy Sciences, Division of Chemical, Biological and Geosciences. The authors also thank Dr Roger Ristau for collecting ESEM images, and Dr You-Jun Fu, Dr Martha Morton, Jennifer Holcolm, Jane Li, and Saminda Dharmarathna for their assistance in the use of the instruments and for helpful discussions.

Notes and references

- O. Platteau and M. Carrillo, Determination of metallic elements in crude oil-water emulsions by flame AAS, *Fuel*, 1995, **74**, 761–767.
- J. G. Speight, *The Chemistry and Technology of Petroleum*, 4th ed., CRC Press, Boca Raton, FL, 2007, pp. 179–193.
- D. Langevin, S. Poteau, I. Hénaut and J. F. Argillier, Crude oil emulsion properties and their application to heavy oil transportation, *Oil Gas Sci. Technol.*, 2004, **59**, 511–521.
- P. S. Daling and T. Storm, Weathering of oils at sea: model/field area comparisons, *Spill Sci. Technol. Bull.*, 1999, **5**, 63–74.
- R. Bongiovanni, E. Borgarello and E. Pelizzetti, Oil spills in the aquatic environment: the chemistry and photochemistry at the water/oil interface, *La Chim. e L'Ind.*, 1989, **71**, 12–17.
- M. G. Ehrhardt, K. Burns and M. C. Bicego, Sunlight-induced compositional alterations in the seawater-soluble fraction of a crude oil, *Mar. Chem.*, 1992, **37**, 53–64.
- D. Mackay and C. D. McAuliffe, Fate of hydrocarbons discharged at sea, *Oil Chem. Pollut.*, 1988, **5**, 1–20.
- N. S. Ahmed, A. M. Nassar, N. N. Zaki and H. K. Gharieb, Stability and rheology of heavy crude oil-in-water emulsion stabilized by an anionic-nonionic surfactant mixture, *Pet. Sci. Technol.*, 1999, **17**, 553–576.
- R. F. Lee, Photo-oxidation and photo-toxicity of crude and refined oils, *Spill Sci. Technol. Bull.*, 2003, **8**, 157–162.
- T. K. Dutta and S. Harayama, Fate of crude oil by the combination of photooxidation and biodegradation, *Environ. Sci. Technol.*, 2000, **34**, 1500–1505.
- R. L. Zioli and W. F. Jardim, Photochemical transformations of water-soluble fraction (WSF) of crude oil in marine waters: A comparison between photolysis and accelerated degradation with TiO_2 using GC-MS and UVF, *J. Photochem. Photobiol. A*, 2003, **155**, 243–252.
- J. Lee and W. Choi, Photocatalytic degradation of *N*-nitrosodimethylamine: Mechanism, product distribution, and TiO_2 surface modification, *Environ. Sci. Technol.*, 2005, **39**, 6800–6807.
- A. Heller and J. R. Brock, Accelerated photooxidative dissolution of oil spills, in *Aquatic and Surface Photochemistry*, G. R. Helz, R. G. Zepp and D. G. Crosby, ed., CRC Press Inc. Boca Raton, FL, 1994, pp. 427–436.
- A. Heller, J. Schwitzgebel and J. G. Ekerdt, *Abstract 2nd International Symposium on New Trends in Photoelectrochemistry*, University of Tokyo, 1994, p. 1.
- R. M. Garrett, I. J. Pickering, C. E. Haith and R. C. Prince, Photooxidation of crude oils, *Environ. Sci. Technol.*, 1998, **32**, 3719–3723.
- J. R. Payne and C. R. Phillips, Photochemistry of petroleum in water, *Environ. Sci. Technol.*, 1985, **19**, 569–579.

17 M. D'Auria, R. Racioppi and V. Velluzzi, Photodegradation of crude oil: liquid injection and headspace solid-phase microextraction for crude oil analysis by gas chromatography with mass spectrometer detector, *J. Chrom. Sci.*, 2008, **46**, 339–344.

18 D. Clausse, F. Gomez, I. Pezon, L. Komunjer and C. Dalmazzone, Morphology characterizations of emulsions by differential scanning calorimetry, *Adv. Colloid Interface Sci.*, 2005, **117**, 59–74.

19 H. C. Genuino, E. C. Njagi, E. Benbow, G. E. Hoag, J. B. Collins and S. L. Suib, Enhancement of the photodegradation of *N*-nitrosodimethylamine (NDMA) in water using amorphous and platinum manganese oxide catalysts, *J. Photochem. Photobiol. A*, 2011, **217**, 284–292.

20 J. L. Rummel, A. M. McKenna, A. G. Marshall, J. R. Eyler and D. H. Powell, The coupling of direct analysis in real time ionization to Fourier transform ion cyclotron resonance mass spectrometry for ultra-high-resolution mass analysis, *Rapid Commun. Mass Spectrom.*, 2010, **24**, 784–790.

21 D. A. Lange, K. Sujata and H. M. Jennings, Characterization of cement–water systems, *Scanning*, 1990, **90**, 75–76.

22 D. J. Stokes, B. L. Thiel and A. M. Donald, Direct observation of water–oil emulsion system in the liquid state by environmental scanning electron microscopy, *Langmuir*, 1998, **14**, 4402–4408.

23 B. Thiel, I. Bache, A. Fletcher, P. Meredith and A. Donald, An improved model for gaseous amplification in the environmental SEM, *J. Microsc.*, 1997, **187**, 143–157.

24 R. G. Mathews and A. M. Donald, Conditions for imaging emulsions in the environmental scanning electron microscope, *Scanning*, 2002, **2**, 75–85.

25 L. L. Schramm, Petroleum Emulsions Basic Principles, in *Emulsions Fundamentals and Applications in the Petroleum Industry*, L. L. Schramm, ed., American Chemical Society, Washington DC, 1992, pp. 1–49.

26 S. Choi, E. Decker, L. Henson, L. Popplewell and D. McClemen, Stability of citral in oil-in-water emulsions prepared with medium-chain triacylglycerols and triacetin, *J. Agric. Food Chem.*, 2009, **57**, 11349–11353.

27 F. Leal-Calderon, V. Schmitt and J. Bibette, *Emulsion Science Basic Principles*, 2nd edn., Springer Science+Business Media, LLC, New York, 2007, p. 148.

28 D. P. Rimmer, A. A. Gregoli, J. A. Hamshar and E. Yildirim, Pipeline Emulsion Transportation for Heavy Oils, in *Emulsions Fundamental and Applications in the Petroleum Industry*, L. L. Schramm, ed., American Chemical Society, Washington DC, 1992, pp. 295–312.

29 M. J. Schick, *Nonionic Surfactants Physical Chemistry*, Surfactant Science Series, Vol. 2, Marcel Dekker, New York, 1966.

30 N. N. Zaki, Surfactant stabilized crude oil-in-water emulsions for pipeline transportation of viscous crude oils, *Colloids Surf. A*, 1997, **125**, 19–25.

31 J. Czarnecki, Water-in-oil emulsions in recovery of hydrocarbons from oil sands, in *Encyclopedic Handbooks of Emulsion Technology*, J. Sjöblom, ed., Marcel Dekker Inc, New York, 2001, pp. 503–504.

32 P. Literathy, S. Haider, O. Samban and G. Morel, Experimental studies on biological and chemical oxidation of dispersed oil in seawater, *Water Sci. Technol.*, 1989, **24**, 845–856.

33 M. Rondón, J. C. Pereira, P. Bouriat, A. Gracia, J. Lachaise and J.-L. Salager, Breaking of water-in-crude-oil emulsions. 2. Influence of asphaltene concentration and diluent nature on demulsifier action, *Energy Fuels*, 2008, **22**, 702–707.

34 N. Shigemoto, R. Al-Maamari, B. Jibril, A. Hiramaya and M. Sueyoshi, Effect of water content and surfactant type on viscosity and stability of emulsified heavy Mukhaizna crude oil, *Energy Fuels*, 2007, **21**, 1014–1018.

35 L. Kong, J. K. Beattie and R. J. Hunter, Electroacoustic determination of size and charge of sunflower oil-in-water emulsions made by high-pressure homogenising, *Chem. Eng. Process.*, 2001, **40**, 421–429.

36 M. Murillo, Z. Benzo, E. Marcano, C. Gomez, A. Garaboto and C. Marin, Determination of copper, iron and nickel in edible oils using emulsified solutions by ICP-AES, *J. Anal. At. Spectrom.*, 1999, **14**, 815–820.

37 W. A. Rowe and K. P. Yates, X-ray fluorescence method for trace metals in refinery fluid catalytic cracking feedstocks, *Anal. Chem.*, 1963, **35**, 368–370.

38 S. Ashrafizadeh and M. Kamran, Emulsification of heavy crude oil in water for pipeline transportation, *J. Pet. Sci. Eng.*, 2010, **71**, 205–211.

39 P. Sebastião and C. Guedes Soares, Modelling the fate of oil spills at sea, *Spill Sci. Technol. Bull.*, 1995, **2**, 121–131.

40 D. E. Nicodem, C. L. B. Guedes and R. J. Correa, Photochemistry of petroleum I. Systematic study of a brazilian intermediate crude oil, *Mar. Chem.*, 1998, **63**, 93–104.

41 P. F. Pesarini, R. G. S. de Silva, R. J. Correa, D. E. Nicodem and N. C. de Lucas, Asphaltene concentration and composition alterations upon solar irradiation of petroleum, *J. Photochem. Photobiol. A*, 2010, **214**, 48–53.

42 R. J. Law, Hydrocarbon concentrations in water and sediments from UK marine waters, determined by fluorescence spectroscopy, *Mar. Pollut. Bull.*, 1981, **12**, 153–157.

43 D. E. Nicodem, C. L. B. Guedes, M. Conceicao, Z. Fernandes, D. Severino, R. J. Correa, M. C. Coutinho and J. Silva, Photochemistry of petroleum, *Progr. Reac. Kinet. Mec.*, 2001, **26**, 219–238.